

Asymmetries in dislocation densities, surface morphology, and strain of GaInAs/GaAs single heterolayers

K. L. Kavanagh,^{a)} M. A. Capano, and L. W. Hobbs
Massachusetts Institute of Technology, Cambridge, Massachusetts 02139

J. C. Barbour
Sandia National Laboratories, Albuquerque, New Mexico 87185

P. M. J. Marée,^{b)}
FOM-Institute for Atomic and Molecular Physics, Kruislaan 407, 1098 S. J. Amsterdam, The Netherlands

W. Schaff and J. W. Mayer
Cornell University, Ithaca, New York 14853

D. Pettit, J. M. Woodall, J. A. Stroschio,^{c)} and R. M. Feenstra
IBM Thomas J. Watson Research Center, Yorktown Heights, New York 10598

(Received 14 March 1988; accepted for publication 29 June 1988)

The dislocation densities, surface morphology, and strain of $\text{Ga}_{1-x}\text{In}_x\text{As}/\text{GaAs}$ epitaxial interfaces as a function of indium composition and layer thickness have been investigated by transmission electron microscopy, medium energy ion blocking, and double-crystal x-ray diffractometry. The electron microscopy shows that in the thinnest dislocated films (90 and 160 nm, $x = 0.07$) $60^\circ \alpha$ dislocations form first in one $\langle 110 \rangle$ direction at the interface. Surprisingly, however, an asymmetry in residual layer strain is not detected in these samples, suggesting that the dislocations have the same Burgers vector or are evenly distributed between two Burgers vectors. Orthogonal arrays of dislocations are observed in films thicker than 300 nm (60° and edge-type, $x = 0.07$). In this case, dislocation densities in each $\langle 110 \rangle$ direction are equal to within experimental error while an asymmetry in in-plane strain is measured (18% and 30% for $x = 0.07$, 300, and 580 nm thick, respectively). An unequal distribution of Burgers vectors of 60° or edge-type dislocations is considered responsible for the strain asymmetry in these thicker samples.

I. INTRODUCTION

The formation of dislocations at lattice-mismatched semiconductor interfaces is a subject of continued attention. Much of the work in this area has been concerned with lattice-mismatched (001) interfaces of diamond cubic or zinc-blende crystals where an orthogonal network of predominantly $60^\circ a/2\langle 110 \rangle$ -type dislocations forms during epitaxial growth. These dislocations are believed to originate by either nucleation and glide from the surface or by multiplication and bending of substrate dislocations already present in the material.¹

In diamond cubic lattices such as Si or Ge 60° -type dislocations are chemically equivalent. In crystals of zinc-blende symmetry, such as III-V semiconductors, dislocations can be associated with either sublattice. The two types, referred to as α and β dislocations, are not chemically equivalent.² Asymmetries in the densities of orthogonal arrays of 60° dislocations have been observed at (100) GaInP and GaAsP/GaAs interfaces.^{3,4} These perpendicular 60° dislocations are of like sign and are α and β dislocations. Abrahams *et al.*

therefore suggested that differences in the nucleation rate or mobility of the two types were responsible for the asymmetries observed. More recently, direct observation by transmission electron microscopy (TEM) of the movement of α and β dislocations has supported this speculation.⁵ Although the dislocation core structures and hence which sublattice each is associated with is still not clear, the velocity of α dislocations was observed to be much greater than that of β dislocations.

We have been concerned with the structural properties of dislocated GaInAs/GaAs interfaces and have observed an asymmetry in dislocation densities, surface morphology, and layer strain in perpendicular $\langle 110 \rangle$ directions. The purpose of this paper is to present the results of an investigation of these interfaces by TEM, optical microscopy, medium-energy ion blocking (MEIB), and double-crystal x-ray diffractometry (DXD).

II. EXPERIMENTAL WORK

The samples consisted of single $\text{Ga}_{1-x}\text{In}_x\text{As}/\text{GaAs}$ interfaces grown by molecular-beam epitaxy at a substrate temperature of 520 or 550 °C, depending on the system. Samples were grown at a uniform In concentration ($x = 0.07$) to thicknesses ranging from 45 to 580 nm, or with a uniform thickness (1 μm) at In compositions ranging

^{a)} Present address: University of California at San Diego, La Jolla, CA 92093.

^{b)} Present address: Nederlandse Philips Bedrijven B.V., 6434 NE Nijmegen, The Netherlands.

^{c)} Present address: National Bureau of Standards, Gaithersburg, MD 20899.

from $x = 0.025$ to 0.2 . In each case a GaAs buffer layer was grown prior to the deposition of the GaInAs. The indium composition and thickness of each sample, as measured by Rutherford backscattering spectroscopy (RBS) or cross-sectional transmission electron microscopy (XTEM), are listed in Table I. The substrate material and all layers were Si doped at concentrations between 10^{17} and 10^{18} atoms/cm³. In one case, a 60- μm lateral gradient in the indium composition was created, ranging from 0 to 0.15, by shadowing the indium beam with a sample clip.

The crystal defect structure of the interfaces was investigated with TEM in plan view and $\langle 110 \rangle$ cross section. Samples for plan-view TEM were prepared by chemical thinning or by mechanical polishing and ion milling (Ar^+ , 4 keV, 50 μA) from the backside of the substrate. Additional thinning of the GaInAs face was necessary with films thicker than approximately 300 nm. Cross sections of interfaces glued face to face with epoxy (Hardman Inc., No. 04005, Belleville, NJ 07109) were thinned by mechanical polishing and ion milling. The TEM observation was carried out with either a JEOL 1200 or 200CX at accelerating voltages of 120 or 200 keV, respectively. Movement or formation of dislocations was not observed in the microscope.

Medium-energy ion blocking (MEIB) and double-crystal x-ray diffractometry (DXD) were used to obtain a direct measurement of the strain in the GaInAs layer. The ion-blocking experiments measured the position of minima in RBS yields of the substrate and the film aligned in $\langle 011 \rangle$ and $\langle 111 \rangle$ crystallographic directions out of the plane of the interface. Figure 1 shows a schematic diagram of the scattering geometry.⁶ The shift in angle of the film-blocking minimum with respect to the substrate-blocking minimum is a direct measure of the lattice strain in the film. In this work, the measurements were made with a 175-keV H^+ beam giving a depth resolution of ± 1 nm. An accurate measurement of strain was possible from the top 30 nm of the sample, where ion-beam steering effects were negligible. To obtain ion-blocking minima from the unstrained substrate, half of each sample was etched to remove the GaInAs. The detector was a toroidal electrostatic analyzer which enabled simultaneous

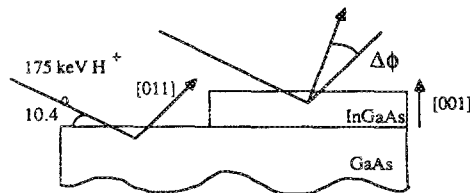


FIG. 1. Scattering geometry for ion-blocking measurements using a 75-keV H^+ beam at an incident random angle of 10.4° to the sample surface.

detection of the backscattered ions as a function of energy and angle over an angular range of 18° . Mechanical movement of the sample was unnecessary except for a vertical translation to select between analysis of the GaInAs or of the exposed substrate. Typically, an ion fluence of 7×10^{14} ions/cm² was required for one measurement. Ion-beam damage was absent in the sample at this dose, as verified with measurements of the yield and position of a blocking minimum for doses up to 1.3×10^{15} ions/cm².

Double-crystal x-ray diffractometry was carried out to measure lattice plane spacings of the film and substrate perpendicular and parallel to the interface. Lattice spacings perpendicular to the interface were measured from rocking curves using the (004) symmetric reflection, while in-plane spacings were determined from $\{224\}$ asymmetric reflections. To separate the component of peak splitting related to lattice tilts caused by misfit dislocations from the components related to elastic strain, rocking curves were recorded from all four $\{224\}$ asymmetric reflections. For both the $\{224\}$ and (004) experiments, a slightly dispersive (+, -) geometry was used with the Si reference crystal oriented to (224) and (004) reflections, respectively. $\text{CuK}\alpha$ radiation produced by a 12-kW rotating anode generator was used in these experiments.

The surface of each sample was studied by optical microscopy with a Nomarski interference attachment and in selected cases by scanning tunneling microscopy (STM). All STM images were acquired with a sample bias of -12.5 V, and a constant tunneling current of 1 nA. The experiments were performed in a low vacuum of about 10^{-7} Torr, and with no sample cleaning prior to imaging. Electrochemically etched tungsten probe tips were used.

TABLE I. Properties of $\text{Ga}_{1-x}\text{In}_x\text{As}/\text{GaAs}$ interfaces measured by RBS and TEM including x , In composition; t , layer thickness; A , asymmetry in interfacial dislocation densities; δ , strain relieved by dislocations assuming them all to be 60° -type; and ϵ_{\parallel}^e , in-plane layer strain equal to f (misfit) $-\delta$.

x	t (nm)	A (%)	δ (%)	ϵ_{\parallel}^e (%)
0.025	1000	20(\pm 20)	0.05(\pm 0.01)	0.13(\pm 0.03)
0.050	1000	15(\pm 15)	0.12(\pm 0.02)	0.24(\pm 0.05)
0.070	45	...	0	0.50
0.070	90	100	0.05(\pm 0.005)	0.45(\pm 0.01)
0.075	160	> 90	0.07(\pm 0.005)	0.47(\pm 0.01)
0.070	300	5(\pm 0.10)	0.13(\pm 0.02)	0.37(\pm 0.05)
0.070	580	7(\pm 0.10)	0.15(\pm 0.02)	0.35(\pm 0.05)
0.070	1000	3(\pm 0.10)	0.18(\pm 0.03)	0.32(\pm 0.05)
0.150	1000	6(\pm 0.15)	0.32(\pm 0.06)	0.53(\pm 0.1)
0.160	1000	4(\pm 0.10)	0.44(\pm 0.07)	0.69(\pm 0.1)

III. RESULTS

A. Transmission electron microscopy

Plan-view and $\langle 011 \rangle$ XTEM micrographs of $\text{Ga}_{0.93}\text{In}_{0.07}\text{As}/\text{GaAs}$ single interfaces are shown in Fig. 2. The GaInAs layer thickness ranged from 45 to 580 nm in these samples. Dislocations are detected in all but the thinnest (45 nm) sample. In each case, it can be seen in the cross-section micrograph that the dislocations are located primarily at one depth in the material, corresponding to the interface depth as measured by RBS. Threading dislocations were rarely observed. In plan view the dislocations are aligned along $\langle 110 \rangle$ directions in the (001) interface plane, essentially randomly distributed in a given direction. There

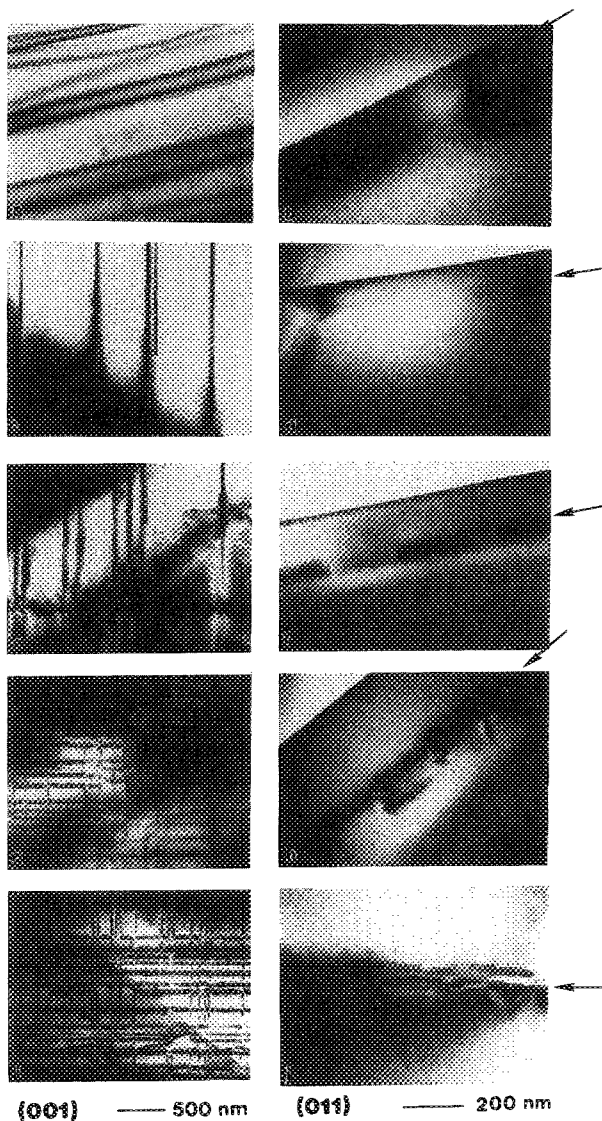


FIG. 2. TEM micrographs of $\text{Ga}_{0.93}\text{In}_{0.07}\text{As}/\text{GaAs}$ interfaces in plan view and $\langle 011 \rangle$ cross section as a function of layer thickness, (a), (b) 45; (c), (d) 90; (e), (f) 160 ($x = 7.5\%$); (g), (h) 300; (i), (j) 580 nm. The arrow in each cross section indicates the interface position.

is a marked asymmetry in the dislocation density (number/cm) in the two $\langle 110 \rangle$ directions in the 90- and 160-nm-thick samples. In fact, dislocations were detected in only one direction in the 90-nm-thick sample. (Two TEM samples were investigated, one fabricated by chemical etching and the other by ion milling. The thinned area in each case was a ring, approximately 0.5 mm in diameter.) An occasional perpendicular dislocation is seen in the 160-nm sample, whereas dislocations in both directions are present in the thicker (300 and 580 nm) samples. Dislocations which form loops above and below the interface can be seen in cross sections in the thicker samples.

Anisotropic etching of a TEM sample from the 90-nm-thick sample showed that the $\langle 110 \rangle$ direction perpendicular to the dislocation line direction produced an undercut etch profile.⁷ If it is assumed that the extra half-plane resides in the GaAs, then the first dislocations that formed were α dislocations.

Orthogonal arrays of dislocations similar to those of the 300- and 580-nm-thick $\text{Ga}_{0.93}\text{In}_{0.07}\text{As}/\text{GaAs}$ were also observed in the 1- μm -thick $\text{Ga}_{1-x}\text{In}_x\text{As}/\text{GaAs}$ samples ($x = 0.025\text{--}0.2$). The interface defect structure of these samples as a function of In concentration is represented well by the one sample grown with a lateral gradient in the indium composition. Figure 3 shows a plan-view TEM micrograph of this sample thinned across the composition gradient. The figure clearly shows that the dislocation density increases laterally as the indium composition or lattice mismatch increases from 0 to 0.15. Note also that in the region of the lowest indium concentration the dislocations are shorter in length, intersecting the surface more frequently. At these smaller strains the formation of the misfit dislocations at the interface by surface nucleation or by bending of threading dislocations may be incomplete.

The average dislocation density D (number/cm) in the two perpendicular $\langle 110 \rangle$ directions for each sample studied was measured from the TEM micrographs. The statistical error in this measurement was determined from the square root of the number of dislocations counted. (This number ranged from 20 to 80 depending on the dislocation density.) The results for D are plotted in Figs. 4(a) and 4(b), as a function of layer thickness and In composition, respectively. The data in Fig. 4(a) show that D increased logarithmically with layer thickness above a certain critical thickness. The critical thickness depended on the interface $\langle 110 \rangle$ direction. Figure 4(b) shows that D increased linearly with In composition ($x = 0.025\text{--}0.20$) in both $\langle 110 \rangle$ directions once an orthogonal array of dislocations had formed.

To obtain a measure of the difference in dislocation densities in the two $\langle 110 \rangle$ directions we define the asymmetry in the dislocation density (A) as half of the difference between the perpendicular densities divided by the average density. The results for A are listed in Table I. An average A of 5% was observed for all samples with In compositions equal to 0.7 or greater and thicknesses greater than 300 nm. An asymmetry as high as 20% was measured for the 0.025 and 0.5 In compositions (1 μm thick). However, in each case these asymmetries were less than the respective statistical errors in the measurement ($\pm 10\%\text{--}20\%$). The only statistically significant values for A in Table I are the asymmetries observed for the 90- and 160-nm-thick samples (0.07 In). The asymmetries observed for these layers were 100% and 90%, respectively.

Figure 5 shows plan-view TEM micrographs of an area of the 580-nm-thick sample (0.7 In) for four imaging conditions, g_{040} , g_{400} , g_{220} , and $g_{\bar{2}20}$. All of the curved dislocations, many of the short dislocations, and some long straight dislocations lose contrast for g_{220} or $g_{\bar{2}20}$. We conclude from this that these dislocations, approximately 10% of the total, are edge type with Burgers vectors $\mathbf{b} = a/2\langle 110 \rangle$ in the plane of the interface. TEM stereograms and cathodoluminescence (CL) studies reported by Fitzgerald *et al.*^{8,9} on similar specimens have indicated that the curved-edge dislocations correspond to those that loop below the interface.

The remaining straight dislocations go partially out of contrast for the g_{400} or g_{040} conditions. This is evidence that these dislocations are 60° -type with Burgers vectors $a/$

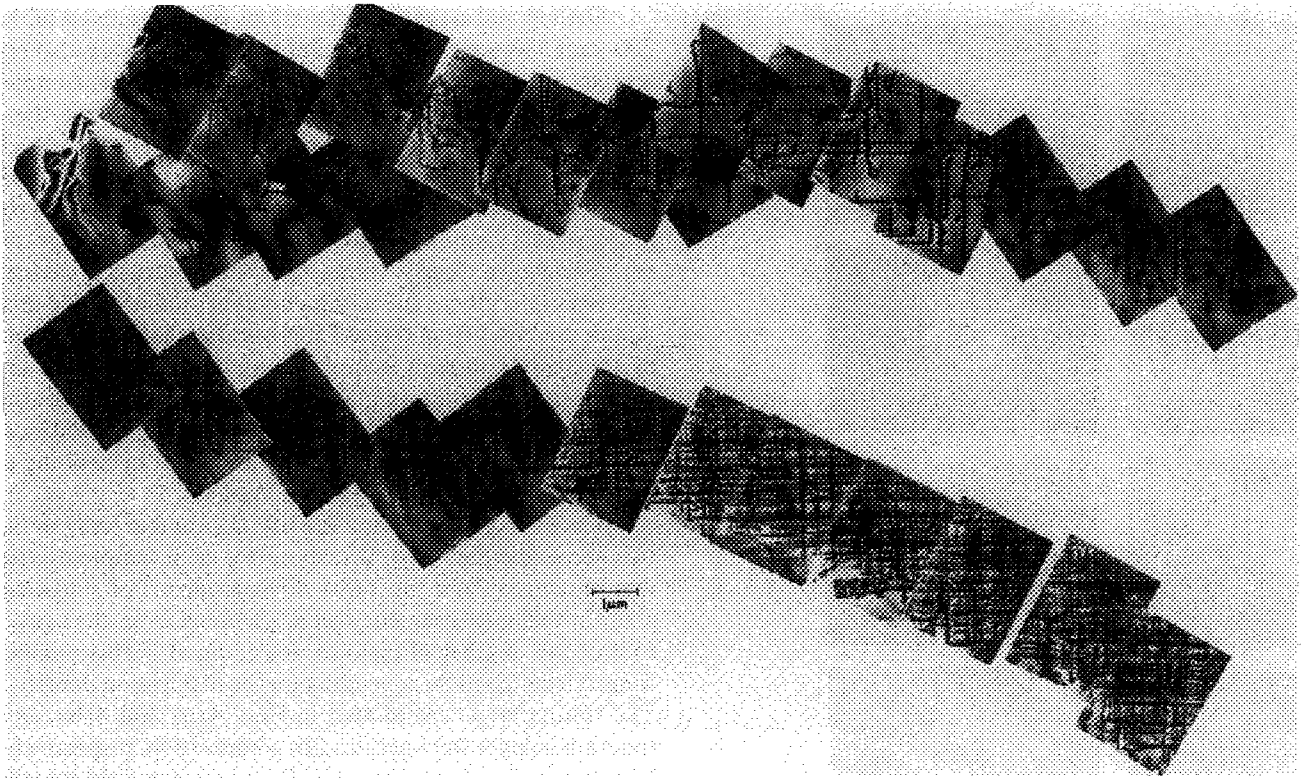
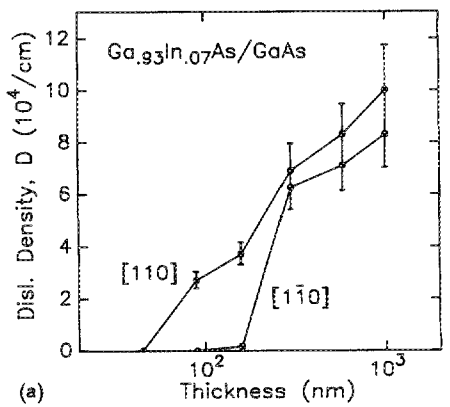
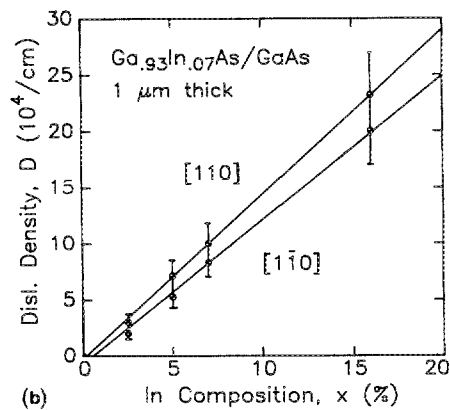


FIG. 3. Plan-view TEM images of a $\text{Ga}_{1-x}\text{In}_x\text{As}/\text{GaAs}$ interface grown with a lateral gradient in the indium composition ranging from $x = 0$ to 0.15.



(a)



(b)

FIG. 4. Average dislocation density D at $\text{Ga}_{1-x}\text{In}_x\text{As}/\text{GaAs}$ interfaces measured from plan-view TEM micrographs plotted vs (a) layer thickness, $x = 0.07$ or 0.075, and (b) composition, $x = 0-0.16$, 1- μm -thick layers.

$2\langle 101 \rangle$ or $a/2\langle 011 \rangle$ out of the plane of the interface. In this case $\mathbf{g} \cdot \mathbf{b} = 0$ and residual contrast occurs presumably from the $\mathbf{g} \cdot (\mathbf{b} \times \mathbf{u})$ contribution (\mathbf{u} is the dislocation line direction). The dislocations are of the same sign with the extra half-plane in the GaAs as evidenced by the uniform direction of the dislocation TEM contrast in Fig. 5. Abrahams *et al.* reached a similar conclusion for dislocations that formed at GaInP/GaAs interfaces.⁴

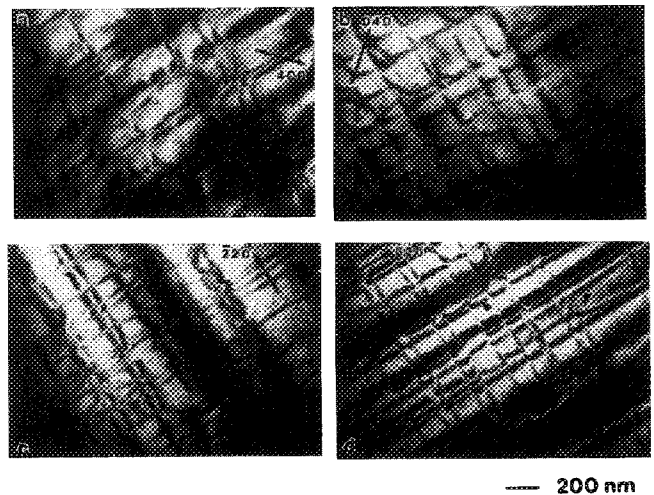


FIG. 5. Plan-view TEM micrographs of a 580-nm-thick dislocated $\text{Ga}_{0.93}\text{In}_{0.07}\text{As}/\text{GaAs}$ interface as a function of the two-beam imaging conditions, g equal to (a) 400, (b) 040, (c) 220, and (d) 220. The pointers in (c) and (d) indicate edge dislocations.

By a similar analysis, the straight dislocations observed in only one direction in the 90- and 160-nm-thick samples were determined to be 60° dislocations. Edge dislocations were not detected in these samples.

The strain relieved by plastic deformation through the formation of dislocations, δ , is equal to $|\mathbf{b}|D$, where D is equal to the average dislocation density and $|\mathbf{b}|$ is the absolute value of the component of the Burgers vector in the direction of interest. Four possible Burgers vectors exist for each of the 60° -type dislocations in perpendicular $\langle 110 \rangle$ dislocations, as illustrated in Fig. 6. If equal numbers of each 60° Burgers vector formed at the interface then their effective Burgers vector would each consist of an edge component equal to $\frac{1}{2}a[110]$, a magnitude $a/(2\sqrt{2})$ in the plane of the interface. All other components cancel. Edge dislocations comprise only 10% of the total number of dislocations at the interface although they relieve twice the strain of the 60° dislocations. However, if we assume that the 60° dislocations were evenly distributed among the possible Burgers vectors and if we ignore the extra 10% contribution by the edge dislocations, then the strain relieved by each dislocation is equal to $(1/2\sqrt{2})aD$.

Calculations for δ based on these assumptions using the dislocation densities obtained from TEM have been listed with the data in Table I. The residual lattice mismatch or the residual $\langle 110 \rangle$ in-plane strain relative to the film, ϵ_{\parallel}^r , is equal to $f(\text{mismatch}) - \delta$. This value, also listed in Table I, will be used later for comparison with the ion-blocking and DXD results.

B. Surface corrugations

It has been known for many years that a corrugated morphology forms on the surface of dislocated interfaces.¹⁰ This surface roughness can be detected by optical microscopy or by scanning electron microscopy (SEM) and ap-

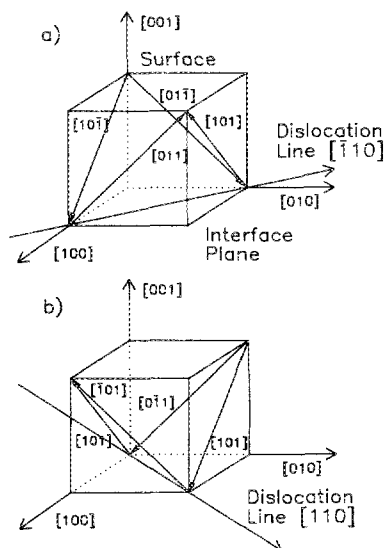


FIG. 6. Schematic diagram showing the possible Burgers vectors of 60° -type dislocations which could form at a (001) GaInAs/GaAs interface in (a) $[110]$ and (b) $[\bar{1}\bar{1}0]$ directions.

pears in the form of perpendicular lines on (001) surfaces running in $\langle 110 \rangle$ directions. A Nomarski interference photograph of the surface of a $1\text{-}\mu\text{m}$ -thick $\text{Ga}_{0.85}\text{In}_{0.15}\text{As}/\text{GaAs}$ sample is shown in Fig. 7(a). Comparable to other reports in the literature,⁹⁻¹¹ perpendicular corrugations aligned along $\langle 110 \rangle$ directions can be seen on the surface of this sample. An asymmetry in the perpendicular densities of these corrugations is clearly evident. We also find that interfaces with a higher lattice mismatch have a higher density of corrugations and that corrugations are not detected optically either on the surface of pseudomorphic layers or on thinner dislocated samples, such as the 300-nm-thick (0.07 In) sample.

The amplitude of the surface corrugations can be measured with STM. Line scans from a $\langle 110 \rangle$ direction on a $1\text{-}\mu\text{m}$ -thick $\text{Ga}_{0.85}\text{In}_{0.15}\text{As}$ layer on GaAs are shown in Fig. 7(b). The scan extends over a lateral area of $800 \times 800 \text{ nm}^2$ and shows that the amplitude of the surface corrugation is 12 nm in this case.

Fitzgerald has shown by CL and TEM that the surface corrugations are correlated to dark line defects and to the location of unique groups of dislocations at the interface.⁹ The corrugations must develop during growth from surface steps created by dislocation formation at the interface. Asymmetries in their densities are therefore related to asymmetries in dislocation Burgers vectors or types.

A rough surface can also be observed after MBE growth in cases of layers with particularly large lattice mismatches ($x > 0.18$). This type of surface roughness may originate from island growth or other instabilities in the layer which are perhaps unrelated to dislocation formation. Figure 8 shows a TEM plan view and $\langle 110 \rangle$ cross section of a 30-nm-thick $\text{Ga}_{0.80}\text{In}_{0.20}\text{As}/\text{GaAs}$ heterolayer. A rough surface with a peak-to-trough amplitude of 10 nm (about one-third the thickness of the layer thickness) is clearly visible in the cross-section view. The sample growth was epitaxial, but the sample thickness is very nonuniform. An orthogonal array of dislocations was not detected in this sample by conventional bright-field TEM, presumably because of the large lattice mismatch and thickness variations.

C. Ion blocking

Typical data obtained from the ion-blocking experiments are shown in Fig. 9. Plotted in this figure are ion scat-

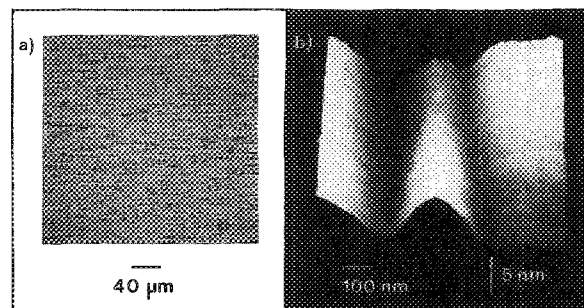


FIG. 7. Surface morphology of a $1\text{-}\mu\text{m}$ -thick $\text{Ga}_{0.85}\text{In}_{0.15}\text{As}/\text{GaAs}$ sample as observed with (a) optical microscopy with a Nomarski attachment and (b) STM line scan in a $\langle 110 \rangle$ direction.

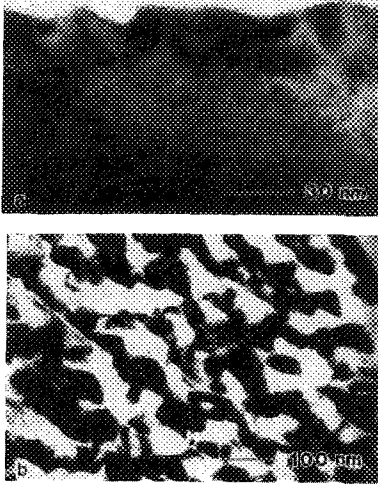


FIG. 8. Bright-field TEM micrographs of a 30-nm-thick $\text{Ga}_{0.80}\text{In}_{0.2}\text{As}/\text{GaAs}$ heterolayer, (a) $\langle 011 \rangle$ cross section and (b) plan view.

tering yields versus angle from the 160-nm-thick $\text{Ga}_{0.93}\text{In}_{0.07}\text{As}$ layer (filled circles) and substrate (open circles). The yield of backscattered ions from the film is greater than the yield from the substrate, and the width of the blocking minima from the film is narrower. Both of these results are expected from the higher scattering factor of the heavier indium atoms in the film. The shifts in minima of the angular scans for the substrate and film were determined from measurement of the average position of the edges at half-height. The error in these numbers depend on statistical fluctuations in the yield and by the degree of asymmetry of the blocking minima.

The angular shift $\Delta\phi$ can be converted to in-plane layer strain relative to the GaInAs , ϵ_{\parallel}^r , by the following geometrical relationship resulting from the tetragonal strain in the epitaxial layer¹²:

$$\Delta\phi = (\epsilon_{\perp}^r - \epsilon_{\parallel}^r) \sin\phi \cos\phi \quad (1)$$

$$= -(1 + \alpha)\epsilon_{\parallel}^r \sin\phi \cos\phi, \quad (2)$$

where ϕ is the angle between the $\langle 001 \rangle$ surface normal and the ion-blocking direction, ϵ_{\perp}^r is the perpendicular strain relative to the film, ϵ_{\parallel}^r is the parallel or in-plane strain relative to the film, and $\alpha = 2(C_{12}/C_{11})$. The elastic parameters C_{12} and C_{11} and the lattice constants of the GaInAs layers were determined by linear interpolation from the bulk values for GaAs and InAs . In this way the expected angular shift in the ion-blocking minima from a $\langle 011 \rangle$ ion-blocking direction for pseudomorphic GaInAs with an indium composition of $0.07 (\pm 0.007)$ is $0.27 (\pm 0.03)^\circ$.

The $\langle 011 \rangle$ ion-blocking results for the series of samples grown with the same indium composition (0.070–0.075), but with layer thicknesses ranging from 45 to 580 nm, are listed in Table II. The angular shift measured for the 45-, 90-, and 160-nm-thick films was $0.32 (\pm 0.02)^\circ$. This is larger than expected, but just within range of experimental error. However, further experiments with improvements in the error might reveal that α is nonlinear at the surface of these films. A plot of film strain in a $\langle 100 \rangle$ interface direction,

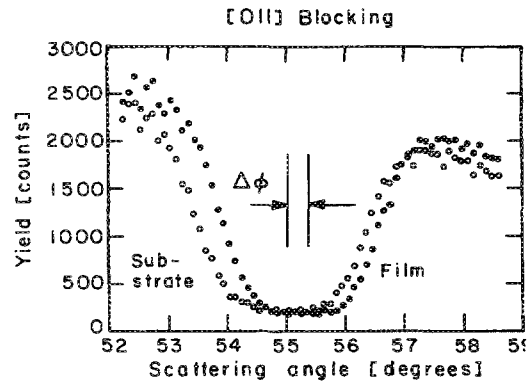


FIG. 9. Scattering yield vs angle near a $\langle 011 \rangle$ ion-blocking direction taken from the film and substrate of a $\text{Ga}_{0.93}\text{In}_{0.07}\text{As}/\text{GaAs}$ (580-nm-thick) interface.

ϵ_{\perp}^r , obtained from this data versus layer thickness is shown in Fig. 10. The data from the 160-nm-thick ($x = 0.075$) film have been normalized to a lattice mismatch of $x = 0.07$ In for comparison with the other layers. A relaxation in strain is detected beginning with the 90-nm-thick film consistent with the formation of dislocations.

Ion-blocking measurements in perpendicular $\langle 111 \rangle$ directions on the same sample were carried out on two layers, $x = 0.07$ (580 nm) and $x = 0.20$ (30 nm). In-plane layer strain parallel to the dislocations along perpendicular $\langle 110 \rangle$ directions, ϵ_{\parallel}^r , was calculated from these data using Eq. (1). The results are listed in Table II with the data from $\langle 011 \rangle$ ion blocking. If the strain was isotropic in the $\langle 001 \rangle$ plane, then the in-plane strain would be the same for $\langle 011 \rangle$ and $\langle 111 \rangle$ ion-blocking directions. However, the strains in perpendicular in-plane $\langle 110 \rangle$ directions for the 580-nm-thick ($x = 0.70$) sample were 0.17 and $0.31 (\pm 0.04)\%$ compared with $0.27 (\pm 0.04)\%$ in the $\langle 100 \rangle$ in-plane direction. Therefore, an asymmetry in the $\langle 110 \rangle$ in-plane strain, A_r , of 29% was detected in the $x = 0.07$ In sample. A similar result was obtained for the $x = 0.20$ sample ($A_r = 19\%$). In both cases the asymmetry is significantly greater than the relative error in the ion-blocking measurements.

D. Double-crystal x-ray diffractometry

Double-crystal x-ray diffractometry (004) rocking curves from $\text{Ga}_{0.93}\text{In}_{0.07}\text{As}/\text{GaAs}$ samples are presented as a function of thickness in Fig. 11. Similar rocking curves were obtained from the $\{224\}$ reflections. The difference in the substrate and layer peak positions, $\Delta\theta$, decreases with thickness. Also, the base of the substrate peak begins to broaden in the 160-nm-thick sample, increasing in width in the 580-nm-thick film to about four times the width of the 45-nm-thick film. The layer peak positions could be measured with an accuracy of ± 12 arcsec corresponding in most cases to an uncertainty in peak separation of less than 5%. The sign convention used is such that a negative $\Delta\theta$ corresponds to the layer peak at an angle smaller than the substrate Bragg angle. A positive $\Delta d/d$ ratio indicates tensile strains or an expansion of the film lattice with respect to the substrate, while compressive strains correspond to a nega-

TABLE II. In-plane strain at GaInAs/GaAs interfaces as measured by medium-energy ion blocking (MEIB).

x	t (nm)	Blocking direction	$\Delta\phi$ (deg)	In-plane direction	ϵ_{\parallel}^x (%)	ϵ_{\parallel}^y (%)	ϵ_{\parallel}^z (%)
0.070	45	$\langle 011 \rangle$	0.33(± 0.02)	$\langle 100 \rangle$	-0.60(± 0.04)	-0.10(± 0.08)	120
0.070	90	$\langle 011 \rangle$	0.31	$\langle 100 \rangle$	-0.56	-0.06	112
0.075	160	$\langle 011 \rangle$	0.32	$\langle 100 \rangle$	-0.58(0.54)	-0.04	107
0.070	300	$\langle 011 \rangle$	0.17	$\langle 100 \rangle$	-0.31	0.19	62
0.070	580	$\langle 011 \rangle$	0.15	$\langle 100 \rangle$	-0.27	0.23	54
0.070	580	$\langle 111 \rangle$	0.09	$\langle 110 \rangle$	-0.17(± 0.04)	0.33(± 0.09)	34
0.070	580	$\langle 111 \rangle$	0.16	$\langle 110 \rangle$	-0.31	0.19	50
$A_r = 29\%$							
0.18	300	$\langle 011 \rangle$	0.22(± 0.03)	$\langle 100 \rangle$	-0.40(± 0.05)	0.88(± 0.1)	27
0.20	30	$\langle 011 \rangle$	0.56(± 0.03)	$\langle 100 \rangle$	-1.00(± 0.05)	0.42(± 0.1)	62
0.20	30	$\langle 111 \rangle$	0.59(± 0.04)	$\langle 110 \rangle$	-1.12(± 0.07)	0.30(± 0.1)	70
0.20	30	$\langle 111 \rangle$	0.40	$\langle 110 \rangle$	-0.76	0.66	47
$A_r = 19\%$							

tive ratio. The peak differentials from the $\{224\}$ rocking curves were tilt corrected by averaging the results obtained from 180° -rotated $\{224\}$ reflections.

In general, $\Delta\theta$ consists of two components: (1) the change in Bragg angle, $\Delta\theta_B$, and (2) the difference in tilt of the substrate and layer planes with respect to the surface, $\Delta\phi$ (identical to the angle measured by ion blocking):¹³

$$\Delta\theta_B = (\epsilon_{\perp}^x \cos^2 \phi + \epsilon_{\parallel}^x \sin^2 \phi) \tan \theta_B, \quad (3)$$

$$\Delta\phi = (\epsilon_{\perp}^x - \epsilon_{\parallel}^x) \sin \phi \cos \phi, \quad (4)$$

$$\Delta\theta = \Delta\theta_B \pm \Delta\phi, \quad (5)$$

where ϕ is the angle of tilt between the lattice planes and the surface, and ϵ_{\perp}^x and ϵ_{\parallel}^x are x-ray strains in the layer measured with respect to the substrate. In our experiments, the angle of incidence of the x ray with the surface was $\theta_B - \phi$, requiring a negative sign in Eq. (5).

With use of Eq. (5), ϵ_{\perp}^x could be calculated directly from the $\langle 004 \rangle$ rocking curves, since in this case $\phi = 0$. Then, knowing $\epsilon_{\perp}^x, \epsilon_{\parallel}^x$ could be calculated from the $\{224\}$ reflec-

tions ($\phi = 35.26^\circ$). The results for ϵ_{\perp}^x and ϵ_{\parallel}^x calculated from Eqs. (2)–(4) are listed in Table III. The results transformed into film strains ϵ_{\perp}^y and ϵ_{\parallel}^y are also listed for comparison with the ion blocking and TEM data in Tables I and II. The data for the 160-nm-thick films ($x = 0.075$) normalized to the mismatch of a $x = 0.07$ In film are listed in parentheses for comparison with the other data.

The result for ϵ_{\perp}^x for the thinnest GaInAs/GaAs sample measured is consistent with a pseudomorphic film of lattice mismatch -0.493% ($x = 0.069$), assuming $\alpha = 0.92$. The absolute measurement error in the concentration (10%) corresponds to an error in lattice mismatch or relative strain of 0.05%. However, the relative error in the composition (2%) plus the DXD measurement error (1%) corresponds to a relative strain error of only 0.015%. This means that the

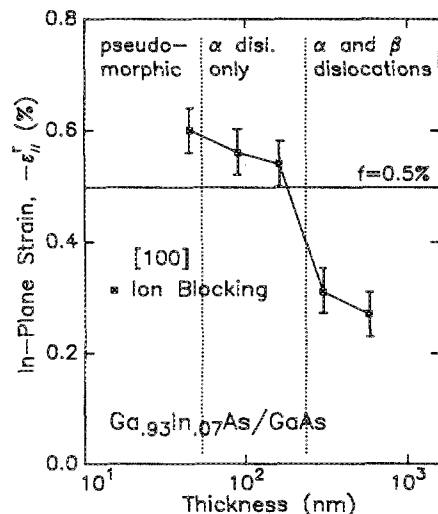


FIG. 10. In-plane strain ϵ_{\parallel}^x in a $\langle 100 \rangle$ direction measured by ion blocking, plotted vs layer thickness for $\text{Ga}_{0.93}\text{In}_{0.07}\text{As}/\text{GaAs}$ interfaces.

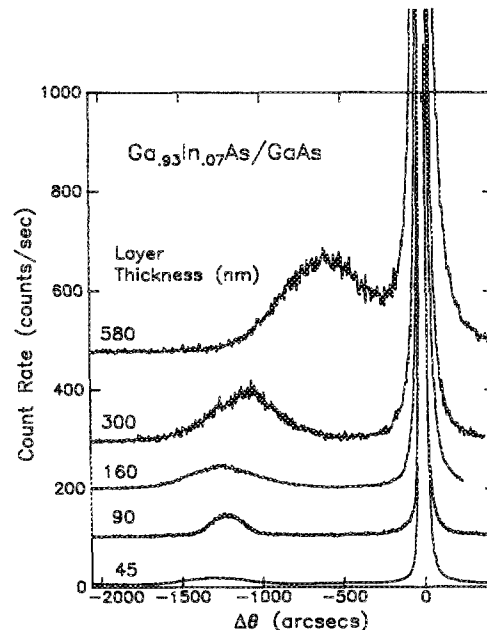


FIG. 11. Double-crystal x-ray rocking curves of the $\langle 004 \rangle$ reflection from $\text{Ga}_{0.93}\text{In}_{0.07}\text{As}/\text{GaAs}$ interfaces as a function of layer thickness.

TABLE III. Perpendicular and in-plane strains at GaInAs/GaAs interfaces as determined by double-crystal x-ray diffractometry (DXD).

t (nm)	$\Delta\theta_{004}$ (arcsec) (± 12)	ϵ_{\perp}^r (%) (± 0.01)	ϵ_{\parallel}^r (%) (± 0.01)	$\Delta\theta_{224}$ (arcsec) (± 24)	ϵ_{\parallel}^i (%) ($\pm 10\%$)	ϵ_{\parallel}^r (%) ($\pm 10\%$)	A_r (%)
45	1280	0.952	FS1.3M 0.449	252	FS1.3M0.001	0.497	.5
90	1220	0.909	FS1.3M 0.406	-260	FS1.3M0.006	0.492	.4
160	-1250	0.930 (0.867)	0.401 (0.365)	224	0.009	0.507	.4
300	-1080	0.805	0.304	-248	0.006	-0.492	0.3
580	-590	0.440	-0.060	-320	0.048	-0.487 (0.45)	18
				-316	0.045	-0.490 (0.46)	18
				-320	0.069	-0.429	CO
				-530	0.201	-0.298	
				-496	0.240	-0.259	
				-688	0.361	-0.139	

relative changes in ϵ_{\parallel}^r greater than 0.015% are significant. A relaxation in perpendicular strain was detected beginning with the 90-nm-thick film consistent with dislocation formation. The formation of defects is also indicated by the broadening in the substrate peak that is observed beginning with the 160-nm-thick layer.

The in-plane strain ϵ_{\parallel}^r is plotted as a function of thickness in Fig. 12. The results for $\Delta\theta$ or ϵ_{\perp}^r in perpendicular $\langle 110 \rangle$ interface directions show that the in-plane strain was symmetric in the 45-, 90-, and 160-nm-thick layers, to within experimental error (24 arcsec), while the in-plane strain of the 300- and 580-nm-thick misfitted samples is asymmetric. Calculations of the strain asymmetry, A_r , from ϵ_{\parallel}^r gave values of 18% and 30% for the 300- and 580-nm-thick samples, respectively.

IV. DISCUSSION

Interfacial dislocations at Ga_{0.93}In_{0.07}As/GaAs interfaces began to form during growth at a layer thickness between 45 and 90 nm. Although in earlier work we did not detect dislocations in a 100-nm-thick sample of the same

composition,¹⁴ these new results are in agreement with the critical thicknesses reported by recent photoluminescence (PL) studies of similar interfaces.¹⁵⁻¹⁷ The critical thickness predicted by anisotropic equilibrium theory at this lattice mismatch for the formation of 60°-type dislocations is 28 nm—lower than the observed range.¹⁸ However, kinetic effects such as dislocation propagation velocities and interactions are not considered in equilibrium calculations. These factors have proven to be important¹⁹ and are probably responsible for the higher critical thicknesses experimentally observed.

In the thinnest films (90 and 160 nm) the dislocations (60° type) formed in only one $\langle 100 \rangle$ direction at the interface. Anisotropic etching of a TEM sample showed that these were α dislocations. Their formation was also detected by DXD and MEIB in the form of a relaxation of tetragonal strain seen by a decrease in the (004) expansion and in the in-plane contraction.

If it is assumed that the α dislocations were evenly distributed among the four possible 60°-type Burgers vectors than the expected in-plane strain relieved in one $\langle 110 \rangle$ direction as calculated from their densities is 0.05–0.07 (± 0.01)% (Table I). (The strain relieved in the perpendicular direction is zero by this assumption.) This value is comparable to the relaxation in in-plane strain of the two films measured by ion blocking in the $\langle 001 \rangle$ interface direction [0.04, 0.06 (± 0.04)%] or by DXD in $\langle 110 \rangle$ directions [0, 0.05 (± 0.05)%]. However, the error on these measurements is large.

DXD results also show that in-plane $\langle 110 \rangle$ strains in the thinner films differed by less than 0.003%–0.015% in the two perpendicular directions rather than the 0.05% suggested by the above analysis. The sensitivity of this measurement was such that a difference greater than 0.02% would have been significant. This result indicates that the α dislocations, instead of being evenly distributed in Burger vector type, had either the same Burgers vector or were evenly distributed between two Burgers vectors. A single 60° dislocation alone or two together, for example, Burgers vectors [101] and [10 $\bar{1}$] in Fig. 6(a), provided both a screw and an edge component at the interface. By either arrangement of 60° dislocations the strain relieved in each $\langle 110 \rangle$ direction would then be equal and the dislocation densities would predict a strain relief of 0.025%.

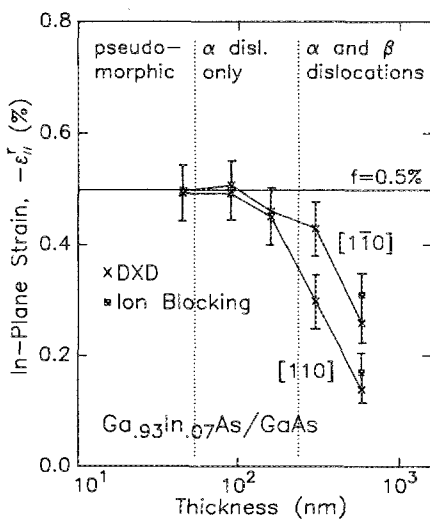


FIG. 12. In-plane strain ϵ_{\parallel}^r in perpendicular $\langle 110 \rangle$ directions for Ga_{0.93}In_{0.07}As/GaAs interfaces plotted vs layer thickness as determined by DXD and ion blocking.

At a layer thickness between 160 and 300 nm β dislocations began to form in the perpendicular $\langle 110 \rangle$ directions, such that an orthogonal array of dislocations was observed. Dislocation densities in the two directions were equal, to within experimental error (10%), yet now a 20%–30% asymmetry in residual layer strain was measured by both MEIB and DXD. Edge dislocations were also observed in these thicker films.

The strain asymmetry in these thicker films can be explained by an uneven distribution of 60° or edge dislocations. This would likewise be consistent with the asymmetries in the surface corrugations observed in the thicker films. An uneven distribution of 60° Burgers vectors would also result in edge components of the plane of the interface and plastic deformation in a direction perpendicular to the interface. The edge dislocations observed which looped above and below the interface are perhaps evidence of this occurring.⁷

The layer strains estimated from dislocation densities in the thicker films were 20% greater than the results measured by MEIB or DXD (300- and 580-nm films). However, the TEM calculation assumed that only 60° -type dislocations were present. This suggests that the contribution made by pure-edge dislocations at the interface to strain relief and asymmetry is greater than 10% and cannot be neglected. Asymmetries in the straight-edge dislocation density at $\text{Ga}_{0.85}\text{In}_{0.15}\text{As}/\text{GaAs}$ interfaces measured by CL and TEM have been reported.⁸ Their formation is thought to occur through the reaction of 60° -type dislocations, a process which would be sensitive to 60° dislocation densities and to α and β identification.

It cannot be determined from our data whether the misfit dislocations formed by nucleation of surface loops and/or by multiplication of threading dislocations. However, threading dislocations have recently been shown to be the dominant nucleation mechanism in $\text{GaInAs}/\text{GaAs}$ when other sources such as surface imperfections are unavailable.¹⁹ In such a case, the multiplication mechanism proposed by Strunk, which results in parallel dislocations with the same Burgers vector,²⁰ might be active in the thinner films and may explain the initial dislocation asymmetry. Alternatively, if surface nucleation is occurring, Marée *et al.* have suggested that partial dislocations are important.²¹ In films under compression (such as $\text{GaInAs}/\text{GaAs}$) the nucleation of 60° dislocations is determined by the rate of nucleation of the 30° partial. Once an asymmetry in strain exists in the film the nucleation of this partial would occur preferentially in one direction and result in an asymmetric array of dislocations. For either of these mechanisms it is expected that the α vs β character of the dislocation will be an important factor. However, further experiments are necessary before the details of this issue will be resolved.

V. CONCLUSIONS

The measurement of strain and dislocation densities at $\text{Ga}_{1-x}\text{In}_x\text{As}/\text{GaAs}$ interfaces as a function of indium composition and layer thickness has been investigated by TEM, medium-energy ion blocking (MEIB), and double-crystal x-ray diffractometry (DXD). TEM studies show that at the thinnest dislocated interfaces ($t = 90$ or 160 nm, $x = 0.07$)

60° α dislocations form first in only one $\langle 001 \rangle$ direction. Surprisingly, an asymmetry in residual strain was not detected by DXD in these samples. In order that the strain is relieved equally in the two in-plane $\langle 110 \rangle$ directions the Burgers vector of these dislocations must therefore be restricted to one or two of the four, possible Burgers vectors.

In the thicker dislocated samples ($t > 300$ nm, $x = 0.07$) orthogonal arrays of dislocations (60° and edge-type) form at the interfaces. Results from both ion blocking and DXD show that the orthogonal array of dislocations is associated with an asymmetry in strain parallel to the interface in perpendicular $\langle 110 \rangle$ directions. This asymmetry is 18% and 30% for 300- and 560-nm-thick $\text{Ga}_{0.93}\text{In}_{0.07}\text{As}/\text{GaAs}$ interfaces, respectively. It is our conclusion that asymmetries in the distribution of 60° Burgers vectors or asymmetries in edge-type dislocation densities were responsible for the strain asymmetry in these thicker samples.

ACKNOWLEDGMENTS

We are grateful to E. A. Fitzgerald (Cornell) and S. Bensoussan (MIT) for many useful discussions and we thank J. Y. Tsao (Sandia) for comments on the manuscript. This work was supported in part by a Bell-Northern Fellowship, a grant from DARPA, and an IBM Post-doctoral Fellowship. We also acknowledge the assistance of R. Coles and M. Craft of the electron-microscope facility of the Cornell Materials Research Center. One of us (J.C.B.) would like to acknowledge support by the U.S. Department of Energy under Contract No. DE-AC04-76DP00789. Part of this work was sponsored by the Stichting voor Fundamenteel Onderzoek der Materie (FOM), with financial support of the Nederlandse Organisatie voor Wetenschappelijk Onderzoek (NWO).

¹P. Petroff, *Inst. Phys. Conf. Ser. No. 23*, 73 (1975).

²M. S. Abrahams, J. Blanc, and C. J. Buiocchi, *Appl. Phys. Lett.* **21**, 185 (1972).

³G. A. Rozgonyi, P. M. Petroff, and M. B. Panish, *J. Cryst. Growth* **27**, 106 (1974).

⁴M. S. Abrahams, L. R. Weisberg, C. J. Buiocchi, and J. Blanc, *J. Mater. Sci.* **4**, 223 (1969).

⁵K.-H. Kuesters, B. C. de Cooman, and C. B. Carter, *Philos. Mag.* **A 53**, 141 (1986).

⁶J. F. van der Veen, *Surf. Sci. Rep.* **5**, 199 (1985).

⁷D. W. Shaw, *J. Cryst. Growth* **47**, 509 (1979).

⁸E. A. Fitzgerald, Y. Ashizawa, L. E. Eastman, and D. G. Ast, *J. Appl. Phys.* **63**, 4965 (1988).

⁹E. A. Fitzgerald, D. G. Ast, P. D. Kirchner, G. D. Pettit, and J. M. Woodall, *J. Appl. Phys.* **63**, 693 (1988).

¹⁰G. Olsen, and M. Ettenberg, *Crystal Growth*, edited by C. H. L. Goodman (Plenum, New York, 1974), Vol. 2, p. 32.

¹¹C. R. Wie and H. M. Kim, *SPIE Proc.* (to be published).

¹²P. M. J. Marée, Olthof, J. W. M. Frenken, J. F. van der Veen, C. W. T. Bulle-Lieuwma, M. P. A. Vieggers, and P. C. Zalm, *J. Appl. Phys.* **58**, 3098 (1985).

¹³V. S. Speriosu and T. Vreeland, *J. Appl. Phys.* **56**, 1591 (1984).

¹⁴J. M. Woodall, G. D. Pettit, K. L. Kavanagh, and J. W. Mayer, *Phys. Rev. Lett.* **51**, 1783 (1983).

¹⁵P. L. Gourley, I. J. Fritz, and L. R. Dawson, *Appl. Phys. Lett.* **52**, 377 (1988).

- ¹⁶T. G. Andersson, Z. G. Chen, V. D. Kulakovskii, A. Uddin, and J. T. Vallin, *Appl. Phys. Lett.* **51**, 752 (1987).
- ¹⁷I. J. Fritz, P. L. Gourley, and L. R. Dawson, *Appl. Phys. Lett.* **51**, 1004 (1987).
- ¹⁸E. A. Fitzgerald and D. G. Ast (unpublished).
- ¹⁹E. A. Fitzgerald, P. D. Kirchner, R. Proano, G. D. Pettit, J. M. Woodall, and D. G. Ast, *Appl. Phys. Lett.* **52**, 1496 (1988).
- ²⁰H. Strunk, W. Hagen, and E. Bauser, *Appl. Phys.* **18**, 67 (1979).
- ²¹P. M. J. Marée, J. F. van der Veen, K. L. Kavanagh, J. C. Barbour, C. W. T. Bulle-Lieuwma, and M. P. A. Vieggers, *J. Appl. Phys.* **62**, 4413 (1987).